


Pulmonary endothelial NEDD9 and the prothrombotic pathophenotype of acute respiratory distress syndrome due to SARS-CoV-2 infection

George A. Alba¹  | Andriy O. Samokhin² | Rui-Sheng Wang² |
Bradley M. Wertheim³ | Kathleen J. Haley³ | Robert F. Padera⁴ |
Sara O. Vargas⁵ | Ivan O. Rosas⁶ | Lida P. Hariri^{1,7} | Angela Shih⁷ |
Boyd Taylor Thompson¹ | Richard N. Mitchell⁴ | Bradley A. Maron²

¹Division of Pulmonary and Critical Care Medicine, Massachusetts General Hospital, Boston, Massachusetts, USA

²Division of Cardiovascular Medicine, Brigham and Women's Hospital, Boston, Massachusetts, USA

³Division of Pulmonary and Critical Care Medicine, Brigham and Women's Hospital, Boston, Massachusetts, USA

⁴Department of Pathology, Brigham and Women's Hospital, Boston, Massachusetts, USA

⁵Department of Pathology, Boston Children's Hospital, Boston, Massachusetts, USA

⁶Division of Pulmonary and Critical Care Medicine, Baylor College of Medicine, Houston, Texas, USA

⁷Department of Pathology, Massachusetts General Hospital, Boston, Massachusetts, USA

Correspondence

Bradley A. Maron, 77 Ave Louis Pasteur, NRB 0630-N, Boston, MA 02115, USA.
Email: bmaron@bwh.harvard.edu

Funding information

Harvard Catalyst, Grant/Award Number: 5KL2TR002542-02; National Institutes of Health, Grant/Award Numbers:

Abstract

The pathobiology of in situ pulmonary thrombosis in acute respiratory distress syndrome (ARDS) due to severe acute respiratory syndrome coronavirus-2 (SARS-CoV-2) infection is incompletely characterized. In human pulmonary artery endothelial cells (HPAECs), hypoxia increases neural precursor cell expressed, developmentally downregulated 9 (NEDD9) and induces expression of a prothrombotic NEDD9 peptide (N_{9p}) on the extracellular plasma membrane surface. We hypothesized that the SARS-CoV-2-ARDS pathophenotype involves increased pulmonary endothelial N_{9p}. Paraffin-embedded autopsy lung specimens were acquired from patients with SARS-CoV-2-ARDS ($n = 13$), ARDS from other causes ($n = 10$), and organ donor controls ($n = 5$). Immunofluorescence characterized the expression of N_{9p}, fibrin, and transcription factor 12 (TCF12), a putative binding target of SARS-CoV-2 and known transcriptional regulator of *NEDD9*. We performed RNA-sequencing on normal HPAECs treated with normoxia or hypoxia (0.2% O₂) for 24 h. Immunoprecipitation-liquid chromatography-mass spectrometry (IP-LC-MS) profiled protein-protein interactions involving N_{9p} relevant to thrombus stabilization. Hypoxia increased TCF12 messenger RNA significantly compared to normoxia in HPAECs in vitro (+1.19-fold, $p = 0.001$; false discovery rate = 0.005), and pulmonary endothelial TCF12 expression was increased threefold in SARS-CoV-2-ARDS versus donor control lungs ($p < 0.001$). Compared to donor controls, pulmonary endothelial N_{9p}-fibrin colocalization was increased in situ in non-SARS-CoV-2-ARDS and SARS-CoV-2-ARDS decedents (3.7 ± 1.2 vs. 10.3 ± 3.2 and 21.8 ± 4.0 arb. units,

George A. Alba and Andriy O. Samokhin are co-first authors.

This is an open access article under the terms of the Creative Commons Attribution-NonCommercial License, which permits use, distribution and reproduction in any medium, provided the original work is properly cited and is not used for commercial purposes.

© 2022 The Authors. *Pulmonary Circulation* published by John Wiley & Sons Ltd on behalf of Pulmonary Vascular Research Institute.

R01HL139613-01, R01HL1535-02,
R01HL155096-01, U54HL119145

$p < 0.001$). However, total pulmonary endothelial N9_p was increased significantly only in SARS-CoV-2-ARDS versus donor controls (15 ± 4.2 vs. 6.3 ± 0.9 arb. units, $p < 0.001$). In HPAEC plasma membrane isolates, IP-LC-MS identified a novel protein-protein interaction between NEDD9 and the β_3 -subunit of the $\alpha_v\beta_3$ -integrin, which regulates fibrin anchoring to endothelial cells. In conclusion, lethal SARS-CoV-2-ARDS is associated with increased pulmonary endothelial N9_p expression and N9_p-fibrin colocalization in situ. Further investigation is needed to determine the pathogenetic and potential therapeutic relevance of N9_p to the thrombotic pathophenotype of SARS-CoV-2-ARDS.

KEYWORDS

acute respiratory distress syndrome, endothelium, pulmonary biology, SARS-CoV-2, thrombosis

INTRODUCTION

Acute respiratory distress syndrome (ARDS) is a highly morbid cause of acute hypoxemic respiratory failure characterized by inflammatory lung injury, in situ pulmonary vascular thrombosis, and microcirculatory dysfunction.¹ Approximately 10%–20% of patients who develop severe infection with severe acute respiratory syndrome coronavirus-2 (SARS-CoV-2), the virus responsible for coronavirus disease 2019 (COVID-19), develop ARDS.^{2–4} Pulmonary vascular dysfunction in ARDS is an independent predictor of mortality.^{5–8} ARDS due to SARS-CoV-2 infection is distinguished by increased pulmonary arteriolar microthrombi and intraluminal fibrin deposition when compared to other forms of ARDS, including pandemic H1N1 influenza.^{9–11} However, studies of thrombotic complications in SARS-CoV-2-ARDS have focused mainly on nonspecific coagulation proteins,¹² thereby hampering insight into pathobiological mechanisms and disease-specific pathogenetic targets.

Neural precursor cell expressed, developmentally downregulated 9 (NEDD9) is a scaffolding protein involved in several important protein-protein interactions.¹³ In human pulmonary artery endothelial cells (HPAECs), NEDD9 is profibrotic,¹⁴ and hypoxia-inducible factor-1 α (HIF1 α) signaling induces expression of a specific NEDD9 peptide (N9_p) that ligands activated platelets to promote pathogenic platelet-endothelial adhesion.¹⁵ Additionally, increased pulmonary endothelial NEDD9 expression is observed in human lung diseases characterized by hypoxia and pulmonary vascular thrombosis, such as pulmonary embolism and chronic thromboembolic pulmonary hypertension.¹⁵ These observations

suggest that increased pulmonary endothelial N9_p expression may be unrecognized in the SARS-CoV-2-ARDS thrombotic pathophenotype.

METHODS

Human lung samples

This study included only excess human lung tissue and was approved by the institutional review board at our institution (IRB #2020P001386, IRB# P00010717) with a waiver of informed consent. Pathologic diagnoses were adjudicated independently by board-certified pathologists (R. F. P., L. P. H., S. O. V., A. S., and R. N. M.). Human lung tissue was obtained from (1) patients with diffuse alveolar damage due to SARS-CoV-2 (“COVID-19 ARDS”) and alternative etiologies (“non-COVID-19 ARDS”) (R. F. P., L. P. H., A. S., and R. N. M.) at the time of autopsy, (2) patients with pulmonary arterial hypertension (PAH) or idiopathic pulmonary fibrosis (IPF) at the time of lung explant or undergoing open lung biopsy for malignancy (I. O. R. and S. O. V.), and (3) discarded donor lung explants provided by the New England Organ Bank (K. J. H.). All human tissue samples were deidentified before analysis. A board-certified pulmonologist (G. A. A.) confirmed each subject with diffuse alveolar damage met the Berlin definition of ARDS.¹⁶ Clinical details of the COVID-19 ARDS and non-COVID-19 ARDS cohorts are summarized in Table 1 and Tables S1 and S2. The nadir partial pressure of oxygen (PaO₂) to a fraction of inspired oxygen (FiO₂) ratio was determined based on the lowest PaO₂ (and corresponding FiO₂) within the first 24 h

TABLE 1 Baseline clinical data of the ARDS cohorts.

Characteristic	COVID-19 ARDS (n = 13)	Non-COVID-19 ARDS (n = 10)	p Value
Age (years)	61 [57–68]	64 [62–67]	0.8
Male sex	9 (69)	9 (90)	0.3
Time between ARDS diagnosis and death (days)	7 [4–8]	9 [3–17]	0.7
Nadir PaO ₂ /FiO ₂ (P/F) ratio	166 [90–222]	147 [89.5–226]	0.8
ARDS severity			
Mild (P/F 200–300)	3 (24%)	3 (30%)	1.0
Moderate (P/F 100–200)	5 (38%)	5 (50%)	0.7
Severe (P/F < 100)	5 (38%)	2 (20%)	0.4
Ventilatory ratio	1.5 (1.4–1.8)	1.35 (1.1–1.5)	0.04

Note: Continuous variables are presented as median and interquartile range [1st–3rd] and categorical data are reported as number (%). Differences between groups for age, sex, time between ARDS diagnosis and death (days), PaO₂ to FiO₂ (P/F) ratio, and ARDS severity were analyzed by two-sample Student *t* test, Fisher's exact test, Mann-Whitney *U* test, and Fisher's exact test, respectively. The bold value indicates statistical significance *p* < 0.05.

Abbreviations: ARDS, acute respiratory distress syndrome; COVID-19, coronavirus-2019; FiO₂, fraction of inspired oxygen; PaO₂, partial pressure fraction of inspired oxygen.

after intubation and admission to the intensive care unit.

in.) – 60 for men or PBW (kg) = 45.5 + 2.3 (height in in.) – 60) for women.¹⁹

Calculation of the ventilatory ratio

Impaired ventilation, as measured by pulmonary dead space, is an important predictor of adverse outcomes in ARDS.⁸ The ventilatory ratio was developed as a simple surrogate for dead space fraction that can be calculated at the bedside^{17,18} by comparing actual measurements of minute ventilation and PaCO₂ with predicted values of minute ventilation and PaCO₂, as defined by the following equation:

$$\frac{\text{minute ventilation (ml/min)} \times \text{PaCO}_2 \text{ (mmHg)}}{\text{predicted body weight (kg)} \times 100 \times 37.5}$$

To calculate the ventilatory ratio, we used the PaCO₂ (mmHg) from an arterial blood gas measured within the first 24 h of intubation and admission to the intensive care unit matched with the corresponding tidal volume (ml) and respiratory rate (breaths per minute) set on the ventilator to calculate the minute ventilation (ml/min). Predicted body weight (PBW) was calculated using the ARDSnet PBW calculator using the formula PBW (kg) = 50 + 2.3 (height in

Histology and immunohistochemistry

Paraffin-embedded lung tissue was cut in cross-section (5 μm thickness). Deparaffinized slides were stained with hematoxylin and eosin (Sigma) for general histologic analysis and Masson's trichrome (Fisher Scientific) to visualize collagen in the distal pulmonary arterioles (diameter, 20–100 μm). To profile key intermediaries involved in NEDD9 signaling, thrombosis, and endothelial dysfunction, immunofluorescence was performed on lung sections using a commercial antibody against the endothelial plasma membrane protein CD31 (Novus Biologicals; NB100-2284), fibrin (Millipore Sigma; MABS2155), and transcription factor 12 (TCF12) (Thermo Fisher Scientific; OTI4D6). Pulmonary microthrombi were defined in this study as collections of fibrin, confirmed by immunofluorescence, that filled the lumens of small pulmonary arteries or capillaries. These data were quantitated as: total number of pulmonary arterioles or capillaries with pulmonary microthrombi (*N*)/total number of vessels visualized at 100 × (*N*) expressed as a percentage.

To visualize the prothrombotic N9_p, we used a custom-made antibody, as reported recently.¹⁴ Images were acquired

using a Confocal Laser Scanning Microscope (ZEISS LSM 800 with Airyscan), and Zen software (ZEISS) was used to visualize images and quantify immunofluorescence intensity including colocalization of two different immunofluorescence signals according to previously published methods.^{14,15} The Z-stack images were acquired at 0.16 μm intervals for at least 2.4 μm at a data depth of 12 bits with a $\times 20$ –63 objective that corresponds to a minimum pixel size of 0.08 μm and processed in Superresolution (3D, Auto) Airyscan mode. The three-dimensional reconstruction images were created using Zen 2 (Blue Edition) software.^{14,15} All quantitative analyses were performed blinded to the etiology of ARDS.

RNA-sequencing (RNA-Seq) analysis

The RNA-Seq results reported in this study are extrapolated from data reported previously by our laboratory, detailed in reference¹⁴. Briefly, using the RNeasy Mini Kit (Qiagen), messenger RNA (mRNA) was isolated from cultured HPAECs treated with normoxia or hypoxia (0.2% O_2) for 24 h. Briefly, the total RNA per sample was quantified using an Agilent 2100 Bioanalyzer instrument with a corresponding Agilent Bioanalyzer RNA Nano assay. The resulting RNA integrity number (RIN) scores and concentrations were considered for qualifying samples to proceed (9.85 ± 0.37 [8.5–10.0 min, max] RIN, $n = 18$). The samples were then normalized to 200 ng of input in 50 μl (4 ng/ μl), and the mRNA was captured using oligo-dT beads as part of the KAPA mRNA HyperPrep workflow. Purified libraries were run on an Agilent 4200 TapeStation instrument with a corresponding Agilent High Sensitivity D1000 ScreenTape assay. The pool was denatured and loaded onto an Illumina NextSeq 500 instrument, with a High-Output 150-Cycle Kit to obtain Paired-End 75 bp reads. The basecall files were demultiplexed and the resulting FASTQ files were used in subsequent analyses. The read count-based gene expression data were normalized based on library complexity and gene variation using the R package EdgeR. Genes were considered significantly differentially expressed if the p value was < 0.05 and the false discovery rate (FDR) was < 0.05 . The FDR was calculated using the Benjamini–Hochberg method. Results are publicly available (GSE163827).¹⁵

Immunoprecipitation-liquid chromatography-mass spectrometry (IP-LC-MS)

For IP-LC-MS, we isolated plasma membrane fractions of HPAEC lysates using a Plasma Membrane Protein Extraction Kit (Abcam, ab65400) according to the manufacturer's

instructions. Magnetic beads (Bio-Rad Protein G *SureBeads*) were resuspended in 100 μl solution (1 mg at 10 mg/ml), magnetized, and serially washed with 1 ml phosphate-buffered saline (PBS) + 0.1% Tween-20 (PBS-T). NEDD9 antibody (Abcam; 18056) was added to the resuspended beads in a final volume of 200 μl and rotated at room temperature for 10 min. The beads were then magnetized and serially washed with 1 ml PBS-T before incubation with the antigen-containing HPAEC plasma membrane lysate (250–500 μl) for 1 h at room temperature. The beads were then serially washed with 1 ml PBS-T, magnetized, incubated with 40 μl 1 \times Laemmli buffer (Bio-Rad) for 10 min at 70°C, and magnetized. The eluent was transferred to a new vial before loading sodium dodecyl sulfate–polyacrylamide gel electrophoresis.²⁰ After staining the gel with Coomassie blue (Bio-Rad), the target bands were excised and prepared for LC-MS to identify protein–protein interactions with plasma membrane NEDD9 according to previously published methods.¹⁵ Peptide sequences (and hence protein identity) were determined by matching protein databases with the acquired fragmentation pattern by the software program Sequest (Thermo Fisher Scientific). For this targeted method, the instrument only activates an ms/ms fragmentation event if one of the m/z values is found within a 6-ppm mass window. All databases include a reversed version of all the sequences and the data were filtered to between a 1%–2% peptide FDR.

Statistical analysis

All continuous variables are reported as mean \pm standard deviation or median and interquartile range [1st–3rd] for normally and non-normally distributed data, respectively. All categorical data are reported as number (%). Continuous variables were analyzed by Student's t test or Mann–Whitney U test according to their distributions based on results of the Shapiro–Wilks test. Categorical variables were analyzed by Fisher's exact test. One-way analysis of variance (ANOVA) was used to compare differences between more than two groups. Post hoc analysis was performed by Tukey's method. Pearson's and Spearman's correlation coefficients are presented for linear regression analyses involving normally and non-normally distributed data, respectively. A $p < 0.05$ and FDR < 0.05 were considered significant. All data analyses were performed using OriginPro 2021b (v9.85).

RESULTS

Individual data points for each result are provided in the Supplemental Data File.

Baseline characteristics of patients with lethal ARDS

Decedents with confirmed ARDS due to SARS-CoV-2 infection ($n = 13$) had a median age of 61 [57–68] years, were predominantly male ($n = 9$, 69%), and had a median nadir $\text{PaO}_2/\text{FiO}_2$ ratio of 166 (90–222). Of these patients, $n = 3$ (24%), $n = 5$ (38%), and $n = 5$ (38%) had mild, moderate, and severe ARDS, respectively, when using the nadir $\text{PaO}_2/\text{FiO}_2$ ratio for classification (Table 1). Decedents with confirmed ARDS due to alternative causes ($n = 10$) had a median age of 64 [62–67] years, were predominantly male ($n = 9$, 90%), and had a median nadir $\text{PaO}_2/\text{FiO}_2$ ratio of 147 (89.5–226). Of these patients, $n = 3$ (30%), $n = 5$ (50%), and $n = 2$ (20%) had mild, moderate, and severe ARDS, respectively, based on nadir $\text{PaO}_2/\text{FiO}_2$ ratio. Causes of ARDS among the non-SARS-CoV-2 control group included bacterial pneumonia ($n = 1$, 10%), influenza A pneumonia ($n = 2$, 20%), sepsis ($n = 2$, 20%), acute exacerbation of interstitial lung disease ($n = 3$, 30%), drug toxicity ($n = 1$, 10%), and pancreatitis ($n = 1$, 10%). There was no statistically significant difference in age, sex, ARDS severity, nadir $\text{PaO}_2/\text{FiO}_2$ ratio, or time (in days) between ARDS diagnosis and death between the two cohorts.

N9_p expression is increased in pulmonary arteriolar microthrombi of SARS-CoV-2-ARDS lungs

A qualitative comparison in vascular phenotype between controls, SARS-CoV-2-ARDS, ARDS from other causes, and PAH/IPF is presented in Figure 1a. Compared to non-SARS-CoV-2-ARDS lungs, SARS-CoV-2-ARDS lungs demonstrated an increased percentage of microthrombi (69 ± 0.2 vs. $55 \pm 0.2\%$ thrombosis, $p < 0.001$) (Figure 1b). Pulmonary endothelial N9_p expression, quantified by N9_p -CD31 colocalization, was increased significantly in SARS-CoV-2-ARDS pulmonary arterioles compared to non-SARS-CoV-2-ARDS and control lungs (15 ± 4.2 vs. 8.6 ± 3.5 vs. 6.3 ± 0.9 arb. units, respectively, $p = 0.004$ by ANOVA with post hoc analysis by Tukey's method) (Figure 2a). Within pulmonary arteriolar microthrombi, we observed that pulmonary endothelial N9_p -fibrin colocalization was increased in SARS-CoV-2-ARDS compared to non-SARS-CoV-2-ARDS and control lungs (22 ± 4.0 vs. 10 ± 1.1 vs. 3.7 ± 1.2 arb. units, respectively, $p < 0.001$) (Figure 2b).

N9_p expression and ventilatory ratio in ARDS

Compared to ARDS of other causes, the ventilatory ratio within the first 24 h of intubation for mechanical ventilation was increased significantly in patients with ARDS due to SARS-CoV-2 infection (1.4 [1.1–1.5] vs. 1.5 [1.4–1.8], $p = 0.04$) (Figure 3a). In patients with ARDS due to SARS-CoV-2 infection, we observed a trend toward a positive correlation between pulmonary endothelial N9_p expression and the ventilatory ratio ($r = +0.53$, $p = 0.05$) (Figure 3b). However, we did not observe a significant association between pulmonary endothelial N9_p expression and the ventilatory ratio in patients with ARDS due to other causes ($r = -0.09$, $p = 0.8$).

Hypoxia-NEDD9 signaling and fibrin-mediated thrombus stabilization

Data from computational analyses in silico identify TCF12 as one of four HPAEC protein binding targets of the SARS-CoV-2 RNA-dependent RNA polymerase protein, Nsp12,²¹ which is part of the viral replicase complex.²² Additionally, the TCF family has been shown to bind *NEDD9* promoter to increase mRNA transcription.²³ Here, RNA-Seq analysis demonstrated that hypoxia increased TCF12 mRNA compared to normoxia in HPAECs in vitro (+1.19-fold, $p = 0.001$; FDR = 0.005) (Figure 4a). Additionally, compared to control lungs, SARS-CoV-2-ARDS lung samples expressed increased endothelial TCF12 in HPAECs in situ (0.2 ± 0.1 vs. 0.9 ± 0.2 arb. units, $p < 0.001$); however, there was no significant difference in TCF12 expression between SARS-CoV-2 and non-SARS-CoV-2-ARDS lung samples (Figure 4b). Taken together with our immunofluorescence data, these observations imply a common pathway that involves hypoxia-TCF12-NEDD9 signaling regulated by hypoxia in HPAECs across all causes of ARDS assessed in this study, but differential regulation of N9_p in association with increased TCF12 in SARS-CoV-2-ARDS.

We have also shown recently that hypoxia regulates important transcriptional responses in HPAECs that affect NEDD9-dependent platelet-endothelial adhesion and collagen III transcription, which are each implicated in thrombosis.^{14,15,24} Microthrombus stabilization, however, requires protein-protein interactions involving integrin anchors. To explore this further, HPAEC plasma membrane fractions were analyzed using IP-LC-MS.

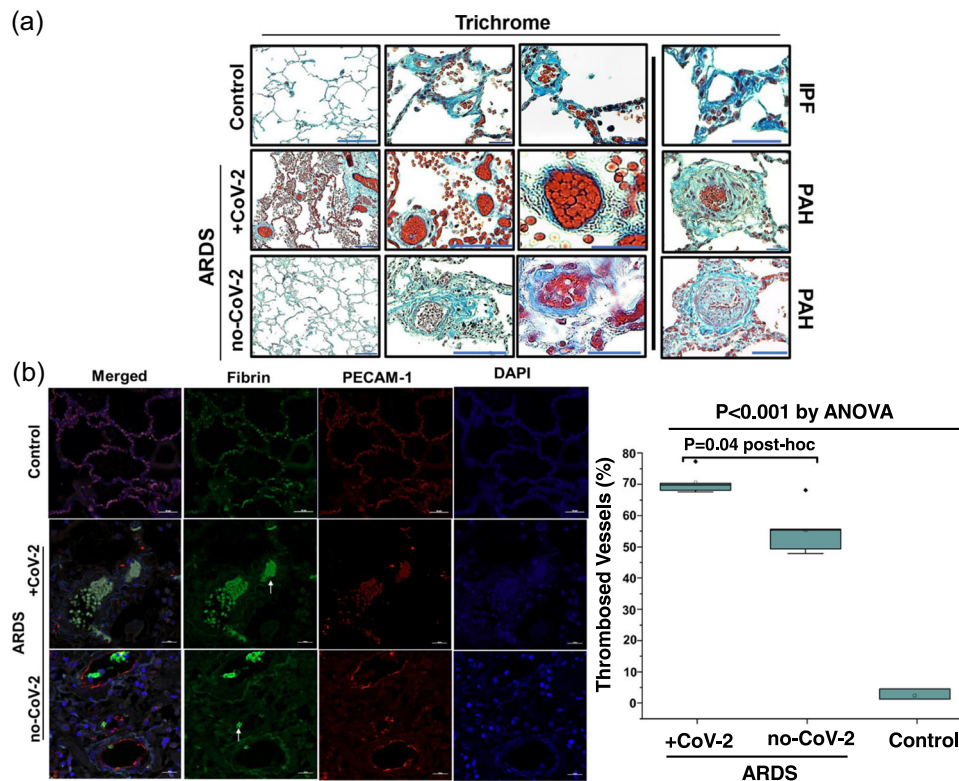


FIGURE 1 Microthrombi are increased in the lungs of patients with ARDS due to SARS-CoV-2 infection. (a) Paraffin-embedded lung sections were obtained at autopsy from donor controls or patients with ARDS and diffuse alveolar damage due to SARS-CoV-2 or non-SARS-CoV-2 causes. Masson trichrome staining was performed to profile global collagen patterns. Pathognomonic findings for macroscopic (organized) thromboembolism are not observed. Representative micrographs shown for $n = 3\text{--}4$ patients/condition. Scale bar = 100 μm . (b) Co-immunofluorescence was performed on human lung sections from controls ($n = 3$), SARS-CoV-2-ARDS ($n = 5$), and non-SARS-CoV-2-ARDS ($n = 5$) using a custom antibody against fibrin and CD31 (also known as platelet endothelial cell adhesion molecule-1 or PECAM-1). Compared to non-SARS-CoV-2-ARDS lungs, SARS-CoV-2-ARDS lungs demonstrated an increased percentage of microthrombi (white arrowheads) (69 ± 0.2 vs. $55 \pm 0.2\%$ thrombosis, $p = 0.004$ by ANOVA post hoc analysis by Tukey's method), which in this study was defined as the total number of pulmonary arterioles or capillaries with intraluminal fibrin/total number of vessels visualized at $\times 100$ expressed as a percentage. Scale bar = 20 μm . ANOVA, analysis of variance; ARDS, acute respiratory distress syndrome; IPF, idiopathic pulmonary fibrosis; PAH, pulmonary arterial hypertension; SARS-CoV-2, severe acute respiratory syndrome coronavirus-2.

From this approach, we identified a novel protein-protein interaction between NEDD9 and the β_3 -subunit of the $\alpha_v\beta_3$ -integrin, which is known to regulate fibrin tethering to endothelial cells (Figure 4c).²⁵

DISCUSSION

In this study of lung tissue from decedents with ARDS, we found that ARDS due to SARS-CoV-2 is associated with increased pulmonary endothelial N9_p expression and N9_p-fibrin colocalization in pulmonary arterial lumens. Additionally, we observed an association between pulmonary endothelial N9_p expression and ventilatory ratio, suggesting a clinically relevant correlation to our histopathophenotypic data linking pulmonary vascular endothelial dysfunction with dead space fraction in SARS-CoV-2 ARDS. Further, we identify a novel

pathway by which NEDD9 may regulate pulmonary microthrombosis: through the formation of a protein-protein complex with β_3 -subunit of the $\alpha_v\beta_3$ -integrin. Overall, findings from this study establish an initial (but much-needed) molecular framework to understand the thrombotic pathophenotype of SARS-CoV-2.

One important finding in our study is the significant increase in the ventilatory ratio among patients with ARDS due to SARS-CoV-2 compared to alternative etiologies. Ventilatory ratio is a simple bedside index to approximate dead space fraction and has been validated in ARDS cohorts.^{17,18} Pulmonary dead-space fraction is one of few lung-specific independent predictors of mortality in ARDS,⁸ but is underutilized clinically. In patients with ARDS due to SARS-CoV-2 infection, increased ventilatory ratios have been observed in patients with elevated D-dimer levels.²⁶ Here, we show

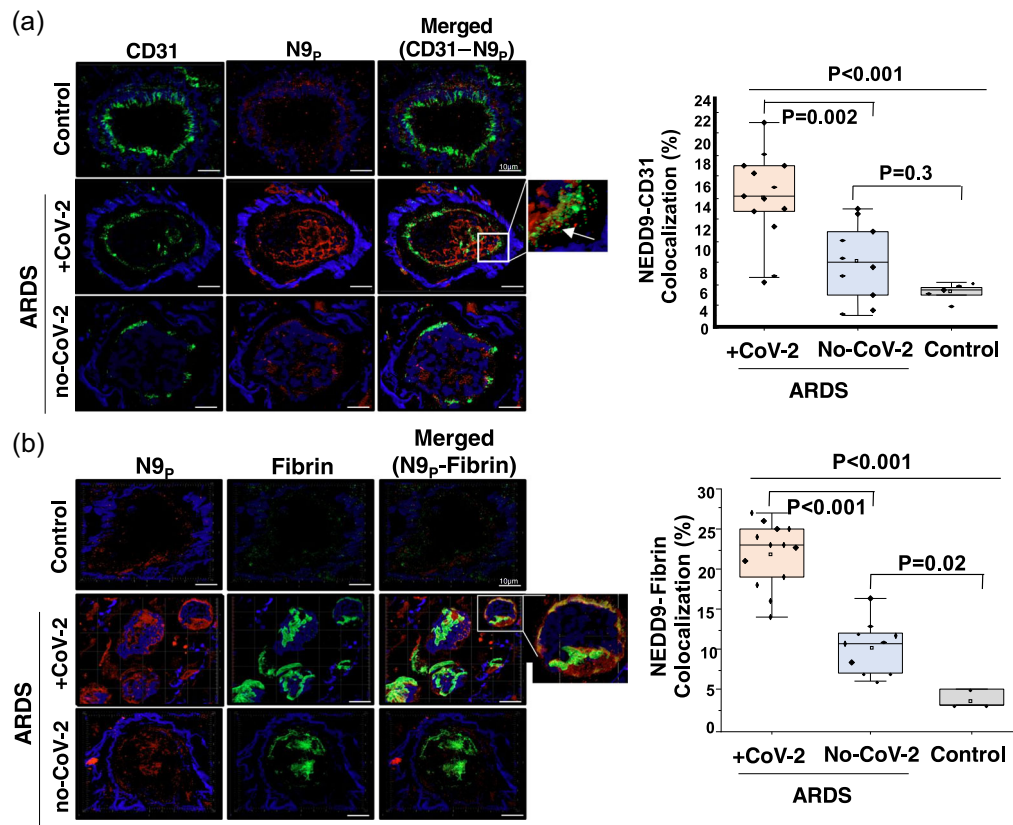


FIGURE 2 The microthrombotic pathophenotype of SARS-CoV-2 ARDS is characterized by increased N9_p. (a) Immunofluorescence was performed on human lung sections from controls ($n = 5$), SARS-CoV-2-ARDS ($n = 13$), and non-SARS-CoV-2-ARDS ($n = 10$) using a custom antibody against a prothrombotic NEDD9 peptide (N9_p) and an antibody against CD31 (with a region of colocalization indicated by the white arrow) and (b) an antibody against fibrin. Representative micrographs are shown. Scale bar = 10 μ m. ARDS, acute respiratory distress syndrome; SARS-CoV-2, severe acute respiratory syndrome coronavirus-2.

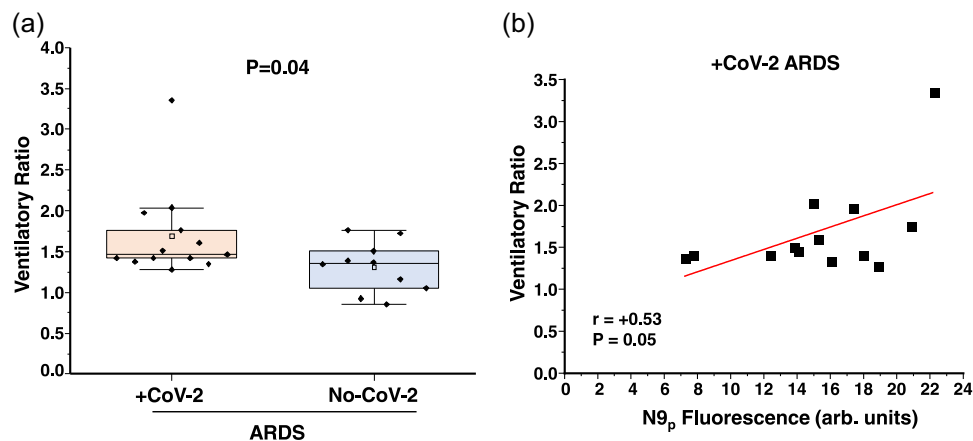


FIGURE 3 Ventilatory ratio is increased in patients with ARDS due to SARS-CoV-2 infection and correlates with pulmonary endothelial N9_p expression. (a) Compared to ARDS of other causes, patients with ARDS due to SARS-CoV-2 infection demonstrated an increased ventilatory ratio within the first 24 h of intubation for mechanical ventilation. (b) In patients with lethal ARDS due to SARS-CoV-2 infection, we observed a moderate positive correlation trend between pulmonary endothelial N9_p expression and the ventilatory ratio. ARDS, acute respiratory distress syndrome; SARS-CoV-2, severe acute respiratory syndrome coronavirus-2.

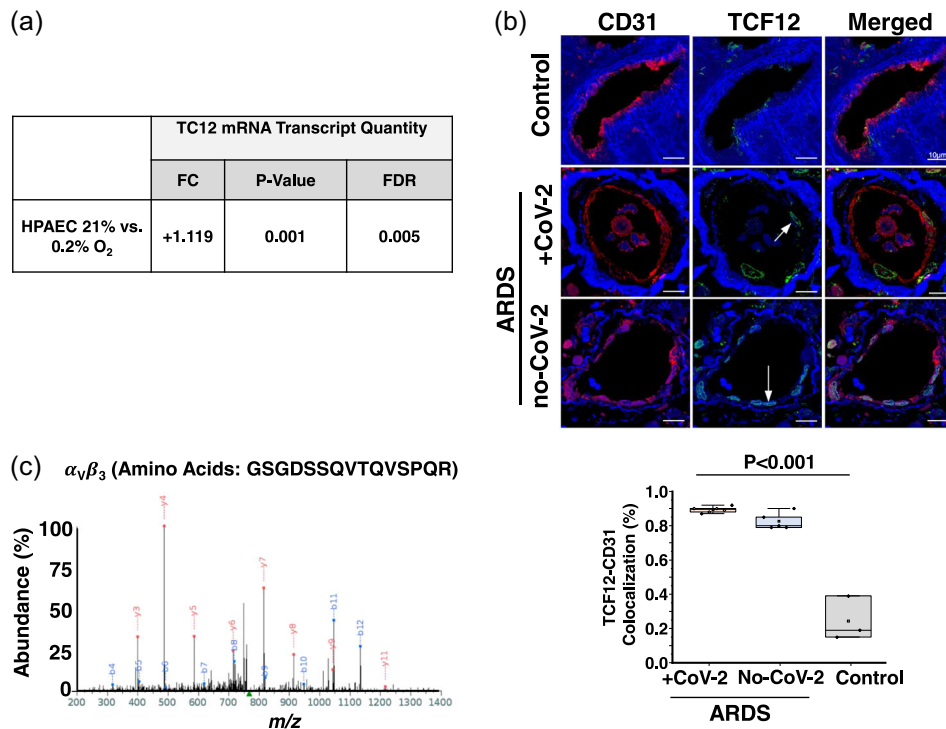


FIGURE 4 Hypoxia–NEDD9 signaling and fibrin-mediated thrombus stabilization. (a) RNA-sequencing analysis demonstrated 24 h of hypoxia (0.2% O₂) increased TCF12 mRNA compared to normoxia (21% O₂) in HPAECs in vitro (+1.19-fold, $p = 0.001$; FDR = 0.005). (b) Immunofluorescence was performed on human lung sections from controls ($n = 3$), SARS-CoV-2–ARDS ($n = 6$), and non-SARS-CoV-2–ARDS ($n = 5$) using an antibody against TCF12 and CD31. Compared to control lungs, SARS-CoV-2–ARDS lungs expressed increased endothelial TCF12 expression (white arrowheads), represented by TCF12–CD31 colocalization. Scale bar = 10 μ m. (c) Anti-NEDD9 immunoprecipitation–mass spectrometry was performed using plasma membrane lysates from cultured human pulmonary artery endothelial cells. The MS2 spectra were obtained at a retention time of 28.65 min and a mass/charge ratio (m/z) value of 766.86863 for the amino acid sequence: GSGDSSQVTQVSPQR, which corresponds to the β_3 -subunit of the $\alpha_v\beta_3$ -integrin. Overall, we identified $n = 4$ sequences for the β_3 -subunit of the $\alpha_v\beta_3$ in a single biological replicate (see Table S3 for details). ARDS, acute respiratory distress syndrome; FDR, false discovery rate; mRNA, messenger RNA; NEDD9, neural precursor cell expressed, developmentally downregulated 9; SARS-CoV-2, severe acute respiratory syndrome coronavirus-2; TCF12, transcription factor 12.

that increased ventilatory ratio in patients with lethal ARDS due to SARS-CoV-2 infection may associate with pulmonary endothelial end-organ damage manifested by elevated N9_p expression and N9_p colocalization with intraluminal fibrin. Future studies are necessary to validate this observation in larger cohorts and determine if specific ARDS subgroups can be identified readily using noninvasive measures of pulmonary endothelial dysfunction, such as plasma NEDD9, to select patients more precisely for antithrombotic therapies or, possibly, emerging anti-NEDD9 therapeutics.¹⁵

We demonstrated previously that in HPAECs, NEDD9 is profibrotic,¹⁴ and hypoxia–HIF-1 α signaling induces expression of a specific N9_p that ligands activated platelets to promote pathogenic platelet–endothelial adhesion.¹⁵ In this study, we demonstrate that N9_p is increased in the pulmonary arteriolar endothelium and intraluminally in patients with lethal ARDS due to SARS-CoV-2 infection

compared to patients with other causes of ARDS. The severity of hypoxemia was similar between the two cohorts, but differential patterns emerged in NEDD9 expression between ARDS due to SARS-CoV-2 and ARDS due to other causes. To account for this observation, we focused on TCF12, which is a proposed binding target of the SARS-CoV-2 RNA-dependent RNA polymerase protein, Nsp12.^{22,23} We demonstrated TCF12 is upregulated by hypoxia in vitro and was consistently increased in the pulmonary endothelium of all patients with ARDS, regardless of etiology. This finding implicates TCF12 in hypoxia signaling in ARDS, but does not explain the increased endothelial N9_p expression observed in ARDS due to SARS-CoV-2 infection, suggesting but not proving that the SARS-CoV-2 viral replicase complex per se may be an important driver of N9_p expression. This observation is, in turn, broadly consistent with other transcriptomic data delineating molecular targets of SARS-CoV-2 from other coronaviruses.⁹

The sample size of this study was small, and most of the patients were male; therefore, generalizing our findings to other COVID-19 populations requires further investigation. Nonetheless, data from affected tissue of COVID-19 patients and ARDS controls has not been widely reported. We did not establish the molecular mechanism by which SARS-CoV-2 may upregulate NEDD9 through TCF12. Because of this, the precise circumstances leading to N9_p bioactivity in patients infected with SARS-CoV-2 are not addressed in this study. Furthermore, most COVID-19 patients do not develop ARDS, although some present clinically with pneumonia and hypoxemia. Since the current study does not address pathobiological factors that explain incident ARDS in COVID-19 patients, it is important to state the true importance of N9_p to the SARS-CoV-2 spectrum of acute lung injury is not established by the current work.

These data suggest that the SARS-CoV-2-ARDS pulmonary vascular pathophenotype is associated with increased N9_p expression and N9_p-fibrin colocalization in HPAECs in situ and increased pulmonary dead-space fraction as approximated by the ventilatory ratio. Increased hypoxia signaling or SARS-CoV-2-mediated regulation of TCF12 are two potential mechanisms by which to explain these findings. These observations suggest that N9_p may represent a novel therapeutic target in patients with pulmonary vascular thrombosis due to SARS-CoV-2-ARDS. However, further investigation is needed to determine the pathogenetic, functional, and therapeutic relevance of N9_p in SARS-CoV-2-mediated pulmonary thrombosis.

AUTHOR CONTRIBUTIONS

George A. Alba, Andriy O. Samokhin, Bradley M. Wertheim, and Bradley A. Maron were responsible for conception and design. George A. Alba, Andriy O. Samokhin, Rui-Sheng Wang, Sara O. Vargas, Boyd Taylor Thompson, and Bradley A. Maron were responsible for the acquisition, analysis, and data interpretation. Kathleen J. Haley, Robert F. Padera, Sara O. Vargas, Ivan O. Rosas, Lida P. Hariri, Angela Shih, and Richard N. Mitchell assisted with pathologic sample acquisition and independent interpretation. George A. Alba, Andriy O. Samokhin, and Bradley A. Maron drafted the article and revised it critically for important intellectual content. All authors edited and approved the final version to be published.

ACKNOWLEDGMENTS

This study is dedicated to the patients and families affected by the COVID-19 pandemic, and all our colleagues on the front lines who helped and cared for them during

unprecedented circumstances. Bradley A. Maron was supported by grants/awards (Nos.: R01HL139613-01, R01HL1535-02, R01HL155096-01), Cardiovascular Medical Research Education Foundation, and McKenzie Family Charitable Trust. George A. Alba was supported by grants/awards (Nos.: 5KL2TR002542-02 and U54HL119145). This study was also conducted with the support of a KL2 award (5KL2TR002542-02) from Harvard Catalyst/The Harvard Clinical and Translational Science Center (National Center for Advancing Translational Sciences, National Institutes of Health Award KL2 TR002542).

CONFLICTS OF INTEREST

George A. Alba: Stock, Verve Therapeutics; Pending US Patents PCT/US2019/059890 and PCT/US2020/066886. Lida P. Hariri: Plaintiff Therapeutics and Boehringer Ingelheim, consulting feeds; Boehringer Ingelheim, medical advisory board. Bradley A. Maron: Actelion; steering committee (outside the scope of this work); Deerfield Company, investigator-sponsored research; Regeneron, consultant (outside the scope of this work); US Patent #9,605,047; PCT/US2015/029672. The remaining authors report no conflicts of interest.

ETHICS STATEMENT

This study included only excess human lung tissue and was approved by the institutional review board at our institution (IRB #2020P001386, IRB# P00010717) with a waiver of informed consent.

ORCID

George A. Alba  <https://orcid.org/0000-0002-6876-7836>

REFERENCES

1. Thompson BT, Chambers RC, Liu KD. Acute respiratory distress syndrome. *N Engl J Med*. 2017;377(6):562–72.
2. Wang D, Hu B, Hu C, Zhu F, Liu X, Zhang J, Wang B, Xiang H, Cheng Z, Xiong Y, Zhao Y, Li Y, Wang X, Peng Z. Clinical characteristics of 138 hospitalized patients with 2019 novel coronavirus-infected pneumonia in Wuhan, China. *JAMA*. 2020;323(11):1061–9.
3. Richardson S, Hirsch JS, Narasimhan M, Crawford JM, McGinn T, Davidson KW, the Northwell COVID- Research C, Barnaby DP, Becker LB, Chelico JD, Cohen SL, Cookingham J, Coppa K, Diefenbach MA, Dominello AJ, Duer-Hefe J, Falzon L, Gitlin J, Hajizadeh N, Harvin TG, Hirschwerk DA, Kim EJ, Kozel ZM, Marrast LM, Mogavero JN, Osorio GA, Qiu M, Zanos TP. Presenting characteristics, comorbidities, and outcomes among 5700 patients hospitalized With COVID-19 in the New York City Area. *JAMA*. 2020;323(20):2052–9.
4. Petrilli CM, Jones SA, Yang J, Rajagopalan H, O'Donnell L, Chernyak Y, Tobin KA, Cerfolio RJ, Francois F, Horwitz LI. Factors associated with hospital admission and critical illness among 5279 people with coronavirus disease 2019 in New

- York City: prospective cohort study. *BMJ*. 2020;369:m1966. <https://doi.org/10.1136/bmj.m1966>
5. Greene R, Lind S, Jantsch H, Wilson R, Lynch K, Jones R, Carvalho A, Reid L, Waltman AC, Zapol W. Pulmonary vascular obstruction in severe ARDS: angiographic alterations after I.V. fibrinolytic therapy. *Am J Roentgenol*. 1987;148(3):501–8.
 6. Zapol WM, Snider MT. Pulmonary hypertension in severe acute respiratory failure. *N Engl J Med*. 1977;296(9):476–80.
 7. Ryan D, Frohlich S, McLoughlin P. Pulmonary vascular dysfunction in ARDS. *Ann Intens Care*. 2014;4:28.
 8. Nuckton TJ, Alonso JA, Kallet RH, Daniel BM, Pittet JF, Eisner MD, Matthay MA. Pulmonary dead-space fraction as a risk factor for death in the acute respiratory distress syndrome. *N Engl J Med*. 2002;346(17):1281–6.
 9. Ackermann M, Verleden SE, Kuehnel M, Haverich A, Welte T, Laenger F, Vanstapel A, Werlein C, Stark H, Tzankov A, Li WW, Li VW, Mentzer SJ, Jonigk D. Pulmonary vascular endothelialitis, thrombosis, and angiogenesis in COVID-19. *N Engl J Med*. 2020;383:120–8.
 10. Hariri LP, North CM, Shih AR, Israel RA, Maley JH, Villalba JA, Vinarsky V, Rubin J, Okin DA, Sclafani A, Alladina JW, Griffith JW, Gillette MA, Raz Y, Richards CJ, Wong AK, Ly A, Hung YP, Chivukula RR, Petri CR, Calhoun TF, Brenner LN, Hibbert KA, Medoff BD, Hardin CC, Stone JR, Mino-Kenudson M. Lung Histopathology in Coronavirus Disease 2019 as compared with severe acute respiratory syndrome and H1N1 influenza: a systematic review. *Chest*. 2021;159(1):73–84. <https://doi.org/10.1016/j.chest.2020.09.259>
 11. Thille AW, Esteban A, Fernández-Segoviano P, Rodriguez JM, Aramburu JA, Vargas-Errázuriz P, Martín-Pellicer A, Lorente JA, Frutos-Vivar F. Chronology of histological lesions in acute respiratory distress syndrome with diffuse alveolar damage: a prospective cohort study of clinical autopsies. *Lancet Respir Med*. 2013;1(5):395–401.
 12. Rodriguez C, Luque N, Blanco I, Sebastian L, Barberà JA, Peinado VI, Tura-Ceide O. Pulmonary endothelial dysfunction and thrombotic complications in patients with COVID-19. *Am J Respir Cell Mol Biol*. 2021;64(4):407–15.
 13. Nikovona AS, Gaponova AV, Kudinov AE, Golemis EA. CAS proteins in health and disease: an update. *IUBMB Life*. 2014;66(6):387–95.
 14. Samokhin AO, Stephens T, Wertheim BM, Wang RS, Vargas SO, Yung LM, Cao M, Brown M, Arons E, Dieffenbach PB, Fewell JG, Matar M, Bowman FP, Haley KJ, Alba GA, Marino SM, Kumar R, Rosas IO, Waxman AB, Oldham WM, Khanna D, Graham BB, Seo S, Gladyshev VN, Yu PB, Fredenburgh LE, Loscalzo J, Leopold JA, Maron BA. NEDD9 targets COL3A1 to promote endothelial fibrosis and pulmonary arterial hypertension. *Sci Transl Med*. 2018;10(445):eaap7294.
 15. Alba GA, Samokhin AO, Wang R-S, Zhang YY, Wertheim BM, Arons E, Greenfield EA, Lundberg Slingsby MH, Ceglowski JR, Haley KJ, Bowman FP, Yu YR, Haney JC, Eng G, Mitchell RN, Sheets A, Vargas SO, Seo S, Channick RN, Leary PJ, Rajagopal S, Loscalzo J, Battinelli EM, Maron BA. NEDD9 is a modifiable mediator of platelet–endothelial adhesion in the pulmonary circulation. *Am J Respir Crit Care Med*. 2021;203:1533–45.
 16. ARDS Definition Task Force, Ranieri VM, Rubenfeld GD, Thompson BT, Ferguson ND, Caldwell E, Fan E, Camporota L, Slutsky AS. Acute respiratory distress syndrome: the Berlin definition. *JAMA*. 2012;307(23):2526–33.
 17. Sinha P, Fauvel NJ, Singh S, Soni N. Ventilatory ratio: a simple bedside measure of ventilation. *Br J Anaesth*. 2009;102(5):692–7.
 18. Sinha P, Calfee CS, Beitler JR, Soni N, Ho K, Matthay MA, Kallet RH. Physiologic analysis and clinical performance of the ventilatory ratio in acute respiratory distress syndrome. *Am J Respir Crit Care Med*. 2019;199(3):333–41.
 19. Acute Respiratory Distress Syndrome Network. Ventilation with lower tidal volumes as compared with traditional tidal volumes for acute lung injury and the acute respiratory distress syndrome. *N Engl J Med*. 2000;342(18):1301–8.
 20. Maron BA, Zhang YY, Handy DE, Beuve A, Tang SS, Loscalzo J, Leopold JA. Aldosterone increases oxidant stress to impair guanylyl cyclase activity by cysteinyl thiol oxidation in vascular smooth muscle cells. *J Biol Chem*. 2009;284:7665–72.
 21. Manalo DJ, Rowan A, Lavoie T, Natarajan L, Kelly BD, Ye SQ, Garcia JGN, Semenza GL. Transcriptional regulation of vascular endothelial cell responses to hypoxia by HIF-1. *Blood*. 2005;105(2):659–69.
 22. Gysi DM, Valle ID, Zitnik M, Ameli A, Gan X, Varol O, Ghiassian SD, Patten JJ, Davey RA, Loscalzo J, Barabási AL. Network medicine framework for identifying drug repurposing opportunities for COVID-19. *Proc Natl Acad Sci USA*. 2021;118(19): e2025581118.
 23. Gordon DE, Jang GM, Bouhaddou M, Xu J, Obernier K, White KM, O’Meara MJ, Rezelj VV, Guo JZ, Swaney DL, Tummino TA, Hüttenhain R, Kaake RM, Richards AL, Tutuncuoglu B, Foussard H, Batra J, Haas K, Modak M, Kim M, Haas P, Polacco BJ, Braberg H, Fabius JM, Eckhardt M, Soucheray M, Bennett MJ, Cakir M, McGregor MJ, Li Q, Meyer B, Roesch F, Vallet T, Mac Kain A, Miorin L, Moreno E, Naing ZZC, Zhou Y, Peng S, Shi Y, Zhang Z, Shen W, Kirby IT, Melnyk JE, Chorba JS, Lou K, Dai SA, Barrio-Hernandez I, Memon D, Hernandez-Armenta C, Lyu J, Mathy CJP, Perica T, Pilla KB, Ganesan SJ, Saltzberg DJ, Rakesh R, Liu X, Rosenthal SB, Calviello L, Venkataramanan S, Liboy-Lugo J, Lin Y, Huang XP, Liu Y, Wankowicz SA, Bohn M, Safari M, Ugur FS, Koh C, Savar NS, Tran QD, Shengjuler D, Fletcher SJ, O’Neal MC, Cai Y, Chang JCI, Broadhurst DJ, Klippsten S, Sharp PP, Wenzell NA, Kuzuoglu-Ozturk D, Wang HY, Trenker R, Young JM, Cavero DA, Hiatt J, Roth TL, Rathore U, Subramanian A, Noack J, Hubert M, Stroud RM, Frankel AD, Rosenberg OS, Verba KA, Agard DA, Ott M, Emerman M, Jura N, von Zastrow M, Verdin E, Ashworth A, Schwartz O, d’Enfert C, Mukherjee S, Jacobson M, Malik HS, Fujimori DG, Ideker T, Craik CS, Floor SN, Fraser JS, Gross JD, Sali A, Roth BL, Ruggero D, Taunton J, Kortemme T, Beltrao P, Vignuzzi M, García-Sastre A, Shokat KM, Shoichet BK, Krogan NJ. A SARS-CoV-2-human protein-protein interaction map reveals drug targets and potential drug repurposing. *Nature*. 2020;583:459–68.

24. Li Y, Bavarva JH, Wang Z, Guo J, Qian C, Thibodeau SN, Golemis EA, Liu W. HEF1, a novel target of Wnt signaling, promotes colonic cell migration and cancer progression. *Oncogene*. 2011;30:2633–43.
25. Stouffer GA, Smyth SS. Effects of thrombin on interactions between beta3-integrins and extracellular matrix in platelets and vascular cells. *Arterioscler Thromb Vasc Biol*. 2003;23(11):1971–8.
26. Grasselli G, Tonetti T, Protti A, Langer T, Girardis M, Bellani G, Laffey J, Carrafiello G, Carsana L, Rizzuto C, Zanella A, Scaravilli V, Pizzilli G, Grieco DL, Di Meglio L, de Pascale G, Lanza E, Monteduro F, Zompatori M, Filippini C, Locatelli F, Cecconi M, Fumagalli R, Nava S, Vincent JL, Antonelli M, Slutsky AS, Pesenti A, Ranieri VM, collaborators. Pathophysiology of COVID-19-associated acute respiratory distress syndrome: a multicentre prospective observational study. *Lancet Respir Med*. 2020;S2213-2600(20):30370–2.

SUPPORTING INFORMATION

Additional supporting information can be found online in the Supporting Information section at the end of this article.

How to cite this article: Alba GA, Samokhin AO, Wang R-S, Wertheim BM, Haley KJ, Padera RF, Vargas SO, Rosas IO, Hariri LP, Shih A, Thompson BT, Mitchell RN, Maron BA. Pulmonary endothelial NEDD9 and the prothrombotic pathophenotype of acute respiratory distress syndrome due to SARS-CoV-2 infection. *Pulmonary Circulation*. 2022;12:e12071. <https://doi.org/10.1002/pul2.12071>